2.3. Real time-PCR

RNA was extracted from sorted and fetal liver samples using a RiboPure™ kit (Life Technologies, Carlsbad, CA) and mRNA was reverse transcribed using a High-Capacity RNA-to-cDNA kit (Life Technologies). cDNA synthesis quality was evaluated by amplifying mouse β-*actin* by PCR. Thirty thermal cycles were employed as follows: denaturation at 95 °C for 10 s, annealing at 60 °C for 20 s, and extension at 72 °C for 20 s. Gene expression levels were measured by real time-PCR with TaqMan® Gene Expression Master Mix and StepOnePlus™ real time PCR (Life Technologies). All probes (*Flt3-L, TPO, EPO, SCF, IL-3, IL-6, IL-11, G-CSF* and *GM-CSF*) were from TaqMan® Gene Expression Assays (Life Technologies). All samples were assayed in triplicate wells. mRNA levels were normalized to β-*actin* and the relative quantity (RQ) of expression was compared with a reference sample.

2.4. Enzyme-Linked Immunosorbent assay (ELISA)

Lysates of sorted cells were obtained using a cell lysis buffer (M-Per® Mammalian Protein Extraction Reagent, Thermo Fisher Scientific, Waltham, MA) containing protease inhibitors (Protease Inhibitor Cocktail, Sigma–Aldrich, St. Louis, MO). The sample was centrifuged at 14000*g* at 4 °C for 15 min. Supernatants containing soluble protein were collected and protein concentration was estimated by measuring absorbance at 280 nm (NANODROP 2000C, Thermo Fisher Scientific). SCF and EPO in sorted cells were assayed using an ELISA kit (Mouse SCF Immunoassay and Mouse EPO Immunoassay, R&D systems) according to the manufacturer's instructions. Experiments were performed in duplicate. The OD was measured using a Thermo Multiskan FC plate reader (Thermo Fisher Scientific).

2.5. Immunohistochemistry

Dissected ICR mouse embryos were fixed in 2% paraformaldehyde in PBS overnight at 4 °C and washed in PBS three times. After 27% sucrose infusion, embryos were embedded in OCT compound (Sakura Finetek, Tokyo, Japan) and frozen in liquid nitrogen (vapor phase). Frozen embryos were sectioned at 20 μm, transferred onto glass slides (Matsunami, Osaka, Japan), and dried. After blocking in 1% BSA in PBS, sections were incubated with primary antibodies overnight at 4 °C. Anti-mouse Dlk-1 Ab (MBL), anti-mouse Lyve-1 Ab (MBL), anti-mouse c-Kit Ab (R&D Systems), anti-mouse SCF Ab (Santa Cruz Biotechnology, Santa Cruz, CA), anti-mouse EPO Ab (Santa Cruz Biotechnology, Santa Cruz, CA) and anti-mouse Ki-67 Ab (Dako Corporation, Carpinteria, CA) served as primary antibodies. After washing in PBS three times, sections stained with Dlk-1, Lyve-1, c-Kit or Ki-67 antibodies were incubated with secondary antibodies and TOTO-3 (Life Technologies) for nuclear staining. In samples stained with SCF or EPO antibodies, the TSA Biotin System (PerkinElmer, Covina, CA) was used to amplify the signal. Donkey anti-rabbit IgG-Alexa555, Donkey anti-goat IgG-Alexa488, Donkey anti-rat IgG-Alexa488 and Alexa546 and

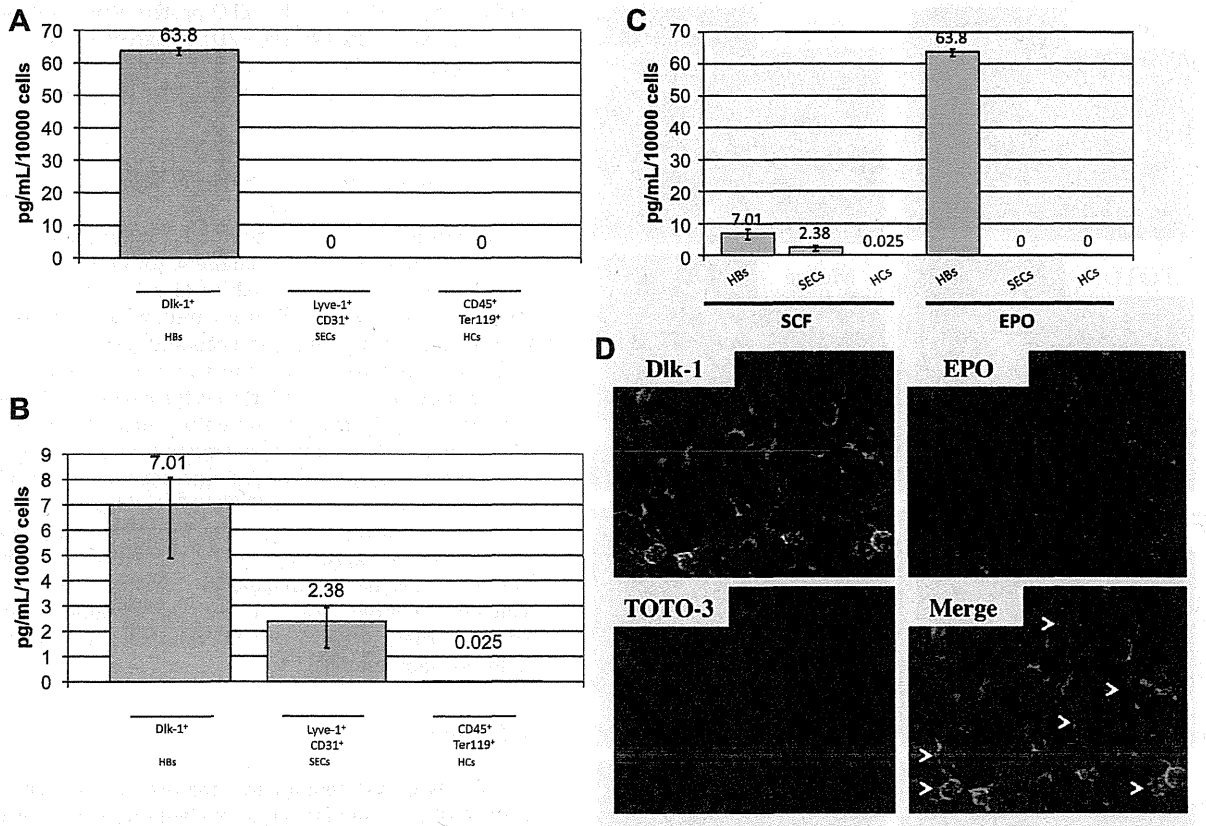

Fig. 2. Expression of EPO and SCF protein in fetal liver. (A) EPO protein in sorted cells was assayed by ELISA. EPO was detected in HBs (63.8 pg/mL/10,000 cells) but not in SECs and HCs at 12.5 dpc. (B) SCF protein in sorted cells was assayed by ELISA. SCF was detected in HBs (7.01 pg/mL/10,000 cells), SECs (2.38 pg/mL/10,000 cells) and HCs (0.025 pg/mL/10,000 cells) at 12.5 dpc. (C) The data from Fig. 2A with 2B were combined to compare EPO and SFC protein expression in each fraction sorted from fetal liver. EPO protein expression was highest in HBs. (D–F) Liver sections were prepared from ICR mouse embryos at 12.5 dpc and stained with Dlk-1 (green), EPO (red) and TOTO-3 (blue) (D); Lyve-1 (green), SCF (red) and TOTO-3 (blue) (E); and Dlk-1 (green), SCF (red) and TOTO-3 (blue) (F). Arrowheads show co-localization of the antigens, respectively. Samples were observed under confocal microscopy. EPO was primarily expressed in HBs expressing Dlk-1, whereas SCF was more widely expressed in FL. Original magnification is 40× (D–F).

Streptavidin Alexa546 (all from Life Technologies) served as secondary antibodies. Coverslips were mounted using fluorescent mounting medium (Dako Corporation, Carpinteria, CA). Slides were observed using a FV-1000 confocal microscope (Olympus, Tokyo, Japan).

2.6. Single cell preparation and cell counting

To prepare single cell suspensions of HCs from *Map2k4*$^{-/-}$ and wild-type FL at 12.5 dpc, dissected FL was crushed on the 40 μm nylon cell strainer (BD Falcon, Bedford, MA) with the inner of 2.5 mL syringe. Cells were washed in PBS and collected into the tube. The number of living cells was counted after Trypan Blue staining.

3. Results

3.1. Cytokine expression in hepatoblasts

We examined expression of several cytokine genes in FL tissue samples at 12.5 and 14.5 dpc using real-time PCR. Significant expression of FMS-like tyrosine kinase 3 ligand (*Flt3l*), thrombopoietin (*TPO*), erythropoietin (*EPO*) and interleukin-6 (*IL-6*) was seen in FL (Fig. 1A). Dlk-1 (Delta-like 1 homolog) is a marker of hepatoblasts (HBs) in FL [16], while Lyve-1 (lymphatic vessel endothelial hyaluronan receptor 1) marks sinusoid endothelial cells (SECs) [17]. As shown in Fig. 1B, fractions of HBs, SECs and hematopoietic cells (HCs) were isolated from mouse FL at both 12.5 and 14.5 dpc by flow cytometry based on expression of the following surface markers: (1) HBs, CD45−/Ter119−/Dlk-1+; (2) SECs, CD45−/Ter119−/Lyve-1+/CD31+; and (3) HCs, CD45+/Ter119+. To determine which component contributes to cytokine production, we used real-time PCR to examine *EPO, Flt3l, IL-6, SCF* and *TPO* expression in isolated HBs, SECs and HCs (Fig. 1C). *EPO* and *TPO* were expressed predominantly in HBs both at 12.5 and 14.5 dpc, suggesting that erythropoiesis and megakaryopoiesis are activated by HBs in FL. Levels of *SCF* mRNA were higher in HBs than in SECs. Expression of *Flt3l* and *IL-6* was predominantly detected in HCs, suggesting that HSCs and HPCs expand via an autocrine mechanism. To investigate expression of the cytokine proteins EPO and SCF, we undertook Enzyme-Linked ImmunoSorbent assay (ELISA) and found that EPO protein was predominantly detected in HBs (63.8 pg/mL/10,000 cells) but was not detected in SECs and HCs (Fig. 2A). SCF protein, however, was detected in all fractions (Fig. 2B). In agreement with *SCF* mRNA expression, HBs expressed SCF protein at a higher level (7.01 pg/mL/10,000 cells) than did SECs (2.38 pg/mL/10,000 cells) or HCs (0.025 pg/mL/10,000 cells). When we compared expression levels of EPO and SCF proteins in each fraction, EPO expression was highest in HBs, suggesting that HBs secrete EPO to regulate FL erythropoiesis (Fig. 2C). To confirm EPO and SCF protein localization in FL, we performed immunohistochemistry and found that EPO protein was expressed primarily in Dlk-1-expressing HBs (Fig. 2D), in agreement with ELISA analysis. Staining of FL with anti-SCF antibody revealed SCF protein in both SECs expressing Lyve-1 and HBs expressing Dlk-1 (Fig. 2E and F).

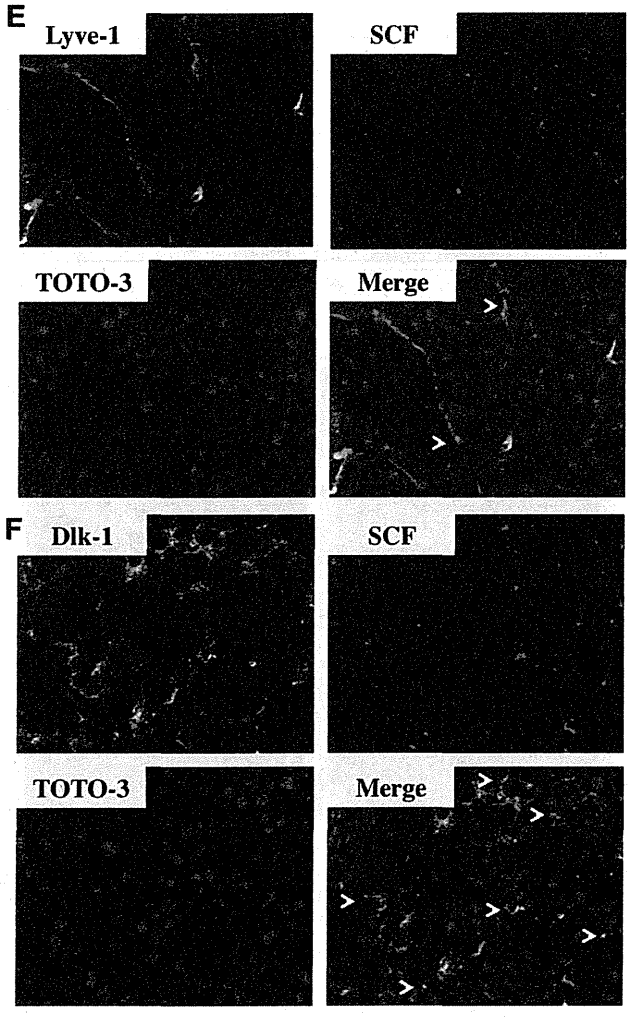

Fig. 2 (*continued*)

3.2. Fetal liver of *Map2k4*$^{-/-}$ mouse embryos

To characterize HB function in FL, we analyzed *Map2k4* (*mitogen-activated protein kinase kinase 4*, formerly known as *Sek1* and *MKK4*)$^{-/-}$ mouse embryos, which lack FL HBs [18–20]. Real-time PCR analysis of whole FL from mutant and wild-type embryos showed that among cytokine-encoding genes, *EPO* and *SCF* mRNAs were down-regulated in the mutant mice, implying an impairment in hematopoiesis, particularly erythropoiesis, in *Map2k4* mutant mice (Fig. 3A). To evaluate potential alterations in hematopoiesis, we performed immunohistochemistry and found that the number of c-Kit expressing cells which represent HSCs and HPCs in the FL at this stage, decreased in a FL field from *Map2k4*$^{-/-}$ mouse embryo relative to wild-type embryo (Fig. 3B; green) [23]. In addition, the number of cells expressing Ki-67, a marker of cell proliferation, decreased in a FL field from *Map2k4*$^{-/-}$ mouse embryos compared to wild-type embryos (Fig. 3B; red). In agreement with the Ki-67 staining, there were fewer FL cells seen in *Map2k4*$^{-/-}$ versus wild-type embryos (Fig. 3C).

4. Discussion

In FL, HSCs differentiate into mature HCs, particularly erythroid cells [9,10]. SCF and EPO are representative cytokines that regulate erythropoiesis [14,15]. Expression levels of *SCF* and *EPO* genes were higher in whole FL tissue than in adult BM and kidney, suggesting that FL primarily functions in erythropoiesis [24]. Recently, using a competitive repopulating assay, Chou and Lodish reported that FL stromal cells expressing both SCF and Dlk-1 support HSC maintenance [25]. However, it remained unclear which cells secreted EPO in FL. HBs are regarded as common progenitors of hepatocytes and biliary epithelial cells and thought to support liver

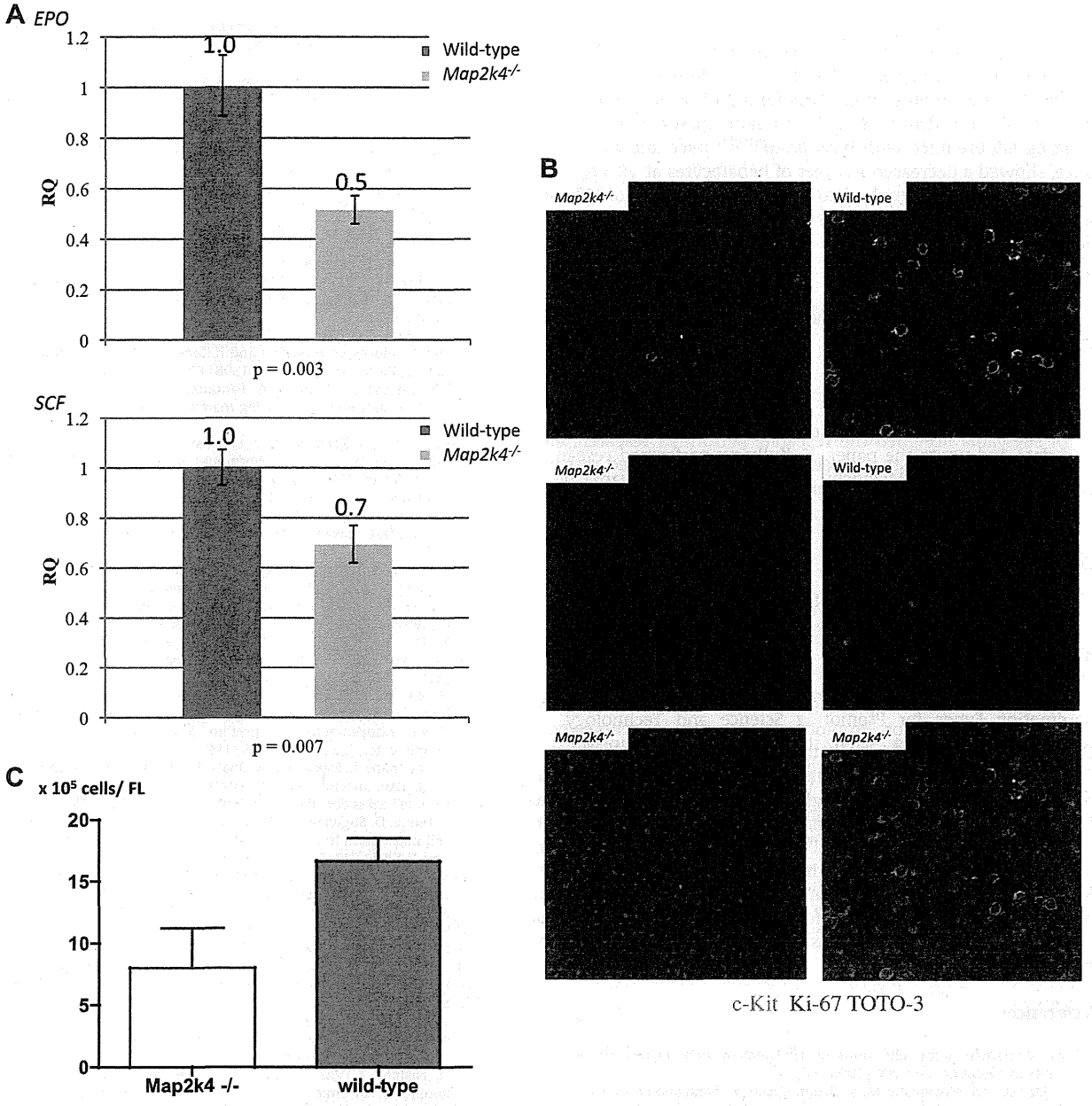

Fig. 3. Phenotypic analysis of FL in *Map2k4*$^{-/-}$ mouse embryos. (A) Expression of *EPO* and *SCF* was examined by real-time PCR in *Map2k4*$^{-/-}$ fetal liver (FL). Expression levels of both *EPO* and *SCF* were down-regulated in *Map2k4*$^{-/-}$ FL relative to wild-type FL. (B) Liver sections were made from both *Map2k4*$^{-/-}$ and wild-type mouse embryos at 12.5 dpc, stained with c-Kit (green), Ki-67 (red) and TOTO-3 (blue), and observed under confocal microscopy. The number of Ki-67 positive cells in a field decreased in *Map2k4*$^{-/-}$ FL compared to wild-type FL. Original magnification is 40×. (C) Single cell suspensions were obtained from *Map2k4*$^{-/-}$ and wild-type FL at 12.5 dpc and the number of living cells was counted after Trypan Blue staining. Significant decreases in the number of *Map2k4*$^{-/-}$ FL cells were observed compared to wild-type FL cells. (For interpretation of the references to color in this figure legend, the reader is referred to the web version of this article.)

construction through formation of a mesh-like structure [16,26]. Our results are strongly indicative of an additional role of HBs in producing erythropoietic cytokines SCF and EPO. Although gene expression of *IL-6* was observed in FL at 12.5 dpc, that was not detected in cell fractions of HBs, SECs and HCs (Fig. 1). As shown in Fig. 1B, we could observe unclassified cell fraction (CD45−/Ter119−/Dlk-1−/Lyve-1−/CD31−), based on surface marker expression, implying that this unclassified cell fraction may express *IL-6* gene. It will be further necessary to clarify roles of the unclassified cells in FL hematopoiesis in the future.

The c-Jun NH_2-terminal protein kinases (JNKs) are members of the mitogen-activated protein kinase (MAPK) family. Map2k4 is a MAPK kinase that directly activates JNKs in response to extracellular and intracellular stresses, and its deficiency leads to abnormal hepatogenesis, resulting in loss of HBs [20,27–29]. In situ hybridization shows that expression of *Map2k4* transcripts is detected in FL by 12.5 dpc and then up-regulated until 16.5 dpc, at which time expression is down-regulated [30]. When *Map2k4*$^{-/-}$ FL cells were transplanted into *rag1*$^{-/-}$ adult mice, both B cells and T cells were generated, demonstrating that *Map2k4*$^{-/-}$ FL cells contain HSCs and/or HPCs [28]. In addition, normal hematopoiesis reportedly occurs in the *Map2k4*$^{-/-}$ YS at both 9.5 and 10.5 dpcs, based on erythroid, myeloid and mixed colony formation [28]. Taken together, hematopoietic potential of *Map2k4*$^{-/-}$ FL looked normal

compared to wild-type mice. Therefore, the decrease of hematopoietic cells were likely due to lack of HBs, but not due to alteration of hematopoietic potential in *Map2k4*$^{-/-}$ FL. Recently, Hikita et al. reported a novel mouse model lacking both HBs and hepatocytes using an *Alb* Cre driver [31]. This mutant mouse, generated by crossing *Alb Cre* mice with both *bcl-xl*$^{flox/flox}$ mice and *mcl-1*$^{flox/flox}$ mice, showed a decreased number of hepatocytes at 18.5 dpc. Future studies will be required to address the function of HBs and hepatocytes in FL erythropoiesis using this model.

5. Conclusion

Hepatoblasts comprise a niche for erythropoiesis through cytokine secretion.

Authorship contributions

D. Sugiyama designed the research, performed research, analyzed data and wrote the paper. K. Kulkeaw performed research and analyzed data. C. Mizuochi, Y. Horio and S. Okayama performed research.

Conflict of interest

The authors have no conflict of interest to declare.

Acknowledgments

The authors acknowledge grant support from the Special Coordination Funds for Promoting Science and Technology, a Grant-in-Aid for Young Scientists (B) from The Ministry of Education, Culture, Sports, Science and Technology, Grant-in-Aid by Ministry of Health, Labor and Welfare, Bilateral Joint Projects for Japan Society for the Promotion of Science, the Ajinomoto Scholarship Foundation and the Tokyo Biochemical Research Foundation. We thank the Research Support Center, the Graduate School of Medical Sciences, Kyushu University, for technical support, Drs. K. Akashi and K. Tani for helpful discussion, Dr. T. Inoue for technical support, and Dr. Elise Lamar for critical reading of the manuscript.

References

[1] I.L. Weissman, Stem cells: units of development, units of regeneration, and units in evolution, Cell 100 (2000) 157–168.
[2] E. Dzierzak, A. Medvinsky, M. de Bruijn, Qualitative and quantitative aspects of hematopoietic cell development in the mammalian embryo, Immunol. Today 19 (1998) 228–236.
[3] S. Matsuoka, K. Tsuji, H. Hisakawa, et al., Generation of definitive hematopoietic stem cells from murine early yolk sac and paraaortic splanchnopleures by aorta–gonad–mesonephros region-derived stromal cells, Blood 98 (2001) 6–12.
[4] D. Sugiyama, K. Tsuji, Definitive hematopoiesis from endothelial cells in the mouse embryo; a simple guide, Trends Cardiovasc. Med. 16 (2006) 45–49.
[5] B.M. Zeigler, D. Sugiyama, M. Chen, Y. Guo, K.M. Downs, N.A. Speck, The allantois and chorion when isolated before circulation or chorio-allantoic fusion, have hematopoietic potential, Development 133 (2006) 4183–4192.
[6] I.M. Samokhvalov, N.I. Samokhvalova, S. Nishikawa, Cell tracing shows the contribution of the yolk sac to adult haematopoiesis, Nature 446 (2007) 1056–1061.
[7] K.E. Rhodes, C. Gekas, Y. Wang, et al., The emergence of hematopoietic stem cells is initiated in the placental vasculature in the absence of circulation, Cell Stem Cell 2 (2008) 252–263.
[8] T. Sasaki, C. Mizuochi, Y. Horio, K. Nakao, K. Akashi, D. Sugiyama, Regulation of hematopoietic cell clusters in the placental niche through SCF/Kit signaling in embryonic mouse, Development 137 (2010) 3941–3952.
[9] G.R. Johnson, R.O. Jones, Differentiation of the mammalian hepatic primordium in vitro. I Morphogenesis and the onset of haematopoiesis, J. Embryol. Exp. Morphol. 30 (1973) 83–96.
[10] G.R. Johnson, M.A. Moore, Role of stem cell migration in the initiation of mouse foetal liver haemopoiesis, Nature 258 (1975) 726–728.
[11] J. Palis, S. Robertson, M. Kennedy, C. Wall, G. Keller, Development of erythroid and myeloid progenitors in the yolk sac and embryo proper of the mouse, Development 126 (1999) 5073–5084.
[12] H. Kurata, G.C. Mancini, G. Alespeiti, A.R. Miqliaccio, G. Miqliaccio, Stem cell factor induces proliferation and differentiation of fetal progenitor cell in the mouse, Br. J. Haematol. 101 (1998) 676–687.
[13] P.D. Kingsley, J. Malik, K.A. Fantauzzo, J. Palis, Yolk sac-derived primitive erythroblasts enucleate during mammalian embryogenesis, Blood 104 (2004) 19–25.
[14] H. Lodish, J. Flygare, S. Chou, From stem regulation of red cell production at multiple levels by mutiple hormones, IUBMB Life 62 (2010) 492–496.
[15] G. Molineux, M.A. Foote, S. Elliott, Erythropoietins and Erythropoiesis, Birkhauser, Basel, Switzerland, 2009.
[16] N. Tanimizu, M. Nishikawa, H. Saito, T. Tsujimura, A. Miyajima, Isolation of hepatoblasts based on the expression of Dlk/Pref-1, J. Cell Sci. 116 (2003) 1775–1786.
[17] C. Mouta Carreira, S.M. Nasser, E. di Toamaso, T.P. Padera, Y. Boucher, S.I. Tomarev, R.K. Jain, LYVE-1 is not restricted to the lymph vessels: expression in normal liver blood sinusoids and down-regulation in human liver cancer and cirrhosis, Cancer Res. 61 (2001) 8079–8084.
[18] H. Nishina, K.D. Fischer, L. Radvanyi, et al., Stress-signalling kinase Sek1 protects thymocytes from apoptosis mediated by CD95 and CD3, Nature 385 (1997) 350–353.
[19] H. Nishina, M. Bachmann, A.J. Oliveira-dos-Santos, Impaired CD28-mediated interleukin 2 production and proliferation in stress kinase SAPK/ERK1 kinase (SEK1)/mitogen-activated protein kinase kinase 4 (MKK4)-deficient T lymphocytes, J. Exp. Med. 186 (1997) 941–953.
[20] T. Watanabe, K. Nakagawa, S. Ohata, SEK1/MKK4-mediated SAPK/JNK signaling paticipates in embryonic hepatoblast proliferation via a pathway different from NF-κB-induced anti-apoptosis, Dev. Biol. 250 (2002) 332–347.
[23] T. Inoue, D. Sugiyama, R. Kurita, et al., APOA-1 is a novel marker of erythroid cell maturation from hematopoietic stem cells in mice and humans, Stem Cell Rev. 7 (2011) 43–52.
[24] S.J. England, K.E. McGrath, J.M. Frame, J. Palis, Immature erythroblasts with extensive ex vivo self-renewal capacity emerge from the early mammalian fetus, Blood 117 (2010) 2708–2717.
[25] S. Chou, H.F. Lodish, Fetal liver hepatic progenitors are supportive stromal cells for hematopoietic stem cells, Proc. Natl. Acad. Sci. USA 107 (2010) 7799–7804.
[26] K. Sasaki, Y. Sonoda, Histometrical and three-dimensional analyses of liver hematopoiesis in the mouse embryo, Arch. Histol. Cytol. 63 (2000) 137–146.
[27] S. Ganiatsas, L. Kwee, Y. Fujiwara, A. Perkins, T. Ikeda, M.A. Labow, L.I. Zon, SEK1 deficiency reveals mitogen-activated protein kinase cascade crossregulation and leads to abnormal hepatogenesis, Proc. Natl. Acad. Sci. USA 95 (1998) 6881–6886.
[28] H. Nishina, C. Vaz, P. Billia, et al., Defective liver formation and liver cell apoptosis in mice lacking the stress signaling kinase SEK1/MKK4, Development 126 (1999) 505–516.
[29] X. Wang, A. Destrument, C. Tournier, Physiological roles of MKK4 and MKK7: insights from animal models, Biochim. Biophys. Acta 1773 (2007) 1349–1357.
[30] J.K. Lee, W.S. Hwang, Y.D. Lee, P.L. Han, Dynamic expression of SEK1 suggests multiple roles of the gene during embryogenesis and in adult brain of mice, Brain Res. Mol. Brain Res. 66 (1999) 133–140.
[31] H. Hikita, T. Takehara, S. Shimizu, Mcl-1 and Bcl-xL cooperatively maintain integrity of hepatocytes in developing and adult murine liver, Hepatology 50 (2009) 1217–1226.

Genes to Cells

Cold exposure down-regulates zebrafish pigmentation

Kasem Kulkeaw[1], Tohru Ishitani[2], Takaaki Kanemaru[3], Ognen Ivanovski[1,4], Midori Nakagawa[1], Chiyo Mizuochi[1], Yuka Horio[1] and Daisuke Sugiyama[1]*

[1]*Department of Hematopoietic Stem Cells, SSP Stem Cell Unit, Faculty of Medical Sciences, Kyushu University, Fukuoka, Japan*
[2]*Division of Cell Regulation Systems, Department of Post-Genome Science Center, Medical Institute of Bioregulation, Kyushu University, Fukuoka, Japan*
[3]*Morphology Core Unit, Kyushu University Hospital, Fukuoka, Japan*
[4]*University Clinic of Urology, Medical Faculty, University 'Ss Cyril and Methodius,' Skopje, Macedonia*

Vertebrates use adaptive mechanisms when exposed to physiologic stresses. However, the mechanisms of pigmentation regulation in response to physiologic stresses largely remain unclear. To address this issue, we developed a novel pigmentation model in adult zebrafish using coldwater exposure (cold zebrafish). When zebrafish were maintained at 17 °C, the pigmentation of their pigment stripes was reduced compared with zebrafish at 26.5 °C (normal zebrafish). In cold zebrafish, gene expression levels of *tyrosinase* and *dopachrome tautomerase*, which encode enzymes involved in melanogenesis, were down-regulated, suggesting that either down-regulation of melanin synthesis occurred or the number of melanophores decreased. Both regular and electron microscopic observation of zebrafish skin showed that the number of melanophores decreased, whereas aggregation of melanosomes was not changed in cold zebrafish compared with normal zebrafish. Taken together, we here show that cold exposure down-regulated adult zebrafish pigmentation through decreasing the number of melanophores and propose that the cold zebrafish model is a powerful tool for pigmentation research.

Introduction

Cold temperatures affect many physiologic processes in endothermic animals, such as slowing the rate of enzymatic reactions, reducing diffusion and transport of biologic molecules, inducing protein denaturation and misaggregation, slowing gene transcription and translation, disrupting cytoskeletal structure and altering cell membrane permeability (Sonna *et al.* 2002). In contrast to endothermic animals, ectothermic vertebrates, such as fish, possess multiple adaptation mechanisms that allow them to cope with low temperatures, which are as follows: (i) increasing the quantity of enzymes involved in lipid metabolism (Cossins *et al.* 2002), (ii) increasing pump activity, Na^+/K^+-ATPase activity and oxygen consumption in hepatocytes and kidney cells (Schwarzbaum *et al.* 1992a,b) and (iii) up-regulation of genes related to oxidative stress in the skeletal muscle of fish tails (Malek *et al.* 2004). Environmental temperature has been shown to affect the expression levels of the cold-shock proteins (Al-Fageeh & Smales 2006). Low temperature (17 °C) induces the expression of cold-shock domain (CSD) containing C2 (*csdc2*) gene in zebrafish kidney marrow (KM) (Kulkeaw *et al.* 2010). Csdc2 contains an S1-like CSD, which is widely found in the cold-shock proteins of eukaryotes, prokaryotes and archaea. Although the functions of cold-shock proteins remain unclear, they have been shown to bind mRNA to regulate ribosomal translation, mRNA degradation and rate of transcription termination (Al-Fageeh & Smales 2006). Heat-shock proteins are also related to environmental temperature, and expression of *heat shock protein 8* (*hspa8*) decreases in carp when exposed to coldwater temperature (Ali *et al.* 2003).

Studies of zebrafish (*Danio rerio*), a teleost tropical fish, have enhanced our understanding of human and mouse developmental biology. Easy handling of embryos and a short lifespan make zebrafish a suitable

Communicated by: Shigeru Kondo
**Correspondence*: ds-mons@yb3.so-net.ne.jp

DOI: 10.1111/j.1365-2443.2011.01498.x

model for investigations into cellular differentiation, organ development and gene function via genetic manipulation. Zebrafish have also been used in pigmentation research. For example, studies of pigment cell differentiation during zebrafish development have produced several mutant strains: *albino*^{b1}, *golden*^{b2}, *brass*^{b4}, *sparse*^{b5} (Parichy *et al.* 1999), *leopard*^{t1} (Johnson & Weston 1995) and *panther*^{j4blue} (Parichy *et al.* 2000). These studies show that zebrafish is a useful genetic model for studying developmental biology in the field of pigmentation research. In adult zebrafish, pigment is represented as blue and black stripes running along the body length and fins, separated by silver interstripes. The pigment cells (chromatophores) are localized in the hypodermis. Zebrafish have three types of chromatophores: xanthophores (yellow), reflective iridophores and melanophores (black), in order from superficial to deep. Pigmented melanophore formation in adult zebrafish requires the differentiation from melanoblasts, melanin synthesis and translocation of melanin-containing granules, or melanosomes. Melanoblast differentiation has been extensively studied in fin regeneration, and *kita* and *kit ligand a* (*kitlga*) have been identified as crucial proponents (Rawls & Johnson 2000, 2001). *Microphthalmia-associated transcription factor a* (*mitfa*) also plays an important role, by controlling the expression of genes encoding the melanin-synthesizing enzymes, *tyrosinase* (*tyr*) and *dopachrome tautomerase* (*dct*) (White & Zon 2008). It appears that *mitfa* is an early marker of melanoblast differentiation (Lister *et al.* 1999), followed by *kita* (Parichy *et al.* 1999) and *dct* (Kelsh & Eisen 2000). Nonpigmented melanophore then synthesizes melanin, which is stored in melanosomes. The melanosomes are then distributed throughout the cytoplasm of melanophore. It has been reported that melanin-concentrating and melanocyte-stimulating hormones (MCH and MSH, respectively) control melanosome translocation (Logan *et al.* 2006). Both hormones are synthesized in brain and have antagonist effects. MCH is derived from pro-melanin-concentrating hormone (*pmch*) and causes melanosome aggregation, whereas MSH is derived from proopiomelanocortin a (*pomca*) and causes melanosome dispersion. In addition to hormone, aggregation of melanosome of fish melanophores is controlled by sympathetic neurons (Iwashita *et al.* 2006). However, the mechanisms of pigmentation regulation in response to physiologic and environmental stresses remained ill-defined. Alternative pigmentation models are necessary to address this issue. In response, we here show a novel model in zebrafish using coldwater exposure.

Results

Cold exposure down-regulates skin pigmentation in zebrafish

No significant differences were observed between the two groups of zebrafish before cold exposure (results not shown). On day 3 of exposure of one group to cold water, pigmentation of cold zebrafish (17 °C) began to become slightly paler than that of normal zebrafish (26.5 °C) (Fig. 1A). One week after cold exposure, the pigmentation of the cold zebrafish, particularly tail, became paler than that of the normal zebrafish. After 2 weeks of cold exposure, the zebrafish pigmentation became even paler (Fig. 1A). High-magnification microscopy of the body flanks and tails showed that the melanophores of cold zebrafish appeared as small spots, as opposed to the larger spots of the normal zebrafish that covered wider area (Fig. 1B). We also assessed the changes in pigmentation before and after cold exposure in individual zebrafish. All cold zebrafish became paler than normal zebrafish (Fig. S1 in Supporting Information). To confirm the down-regulation of pigmentation in cold zebrafish, melanin content was measured by spectrophotometer. Melanin content in the body and tail skin of cold zebrafish was 2.7- and 3.5-fold lower than that of normal zebrafish (Fig. 1C). Moreover, to exclude the possibility that the color adaptation to white background occurred in cold zebrafish, we maintained zebrafish in 26.5 °C water inside of the incubator. The light cycle inside of incubator was controlled following the protocol of cold zebrafish maintenance. Two weeks later, the pigmentation of control zebrafish inside of incubator became slightly pale compared with that outside of incubator but was not severely down-regulated compared with cold zebrafish (Fig. 1A).

Cold exposure disrupts growth of zebrafish

The means and standard deviations of body weight and length were calculated from 6 to 7 zebrafish per group, and Student's *t*-test was used to determine statistical significance. There was a tendency that cold zebrafish had lower body weight and length than normal zebrafish at 1, 2 weeks and 7 months (Fig. 1D). Furthermore, abnormal renal tubules and melanophores were observed in the KM of cold zebrafish, but not in normal zebrafish (Fig. 1E, left and middle panels). To exclude the possibility that the abnormal melanophores were in fact melanin-containing macrophages, images of transmission electron microscopy

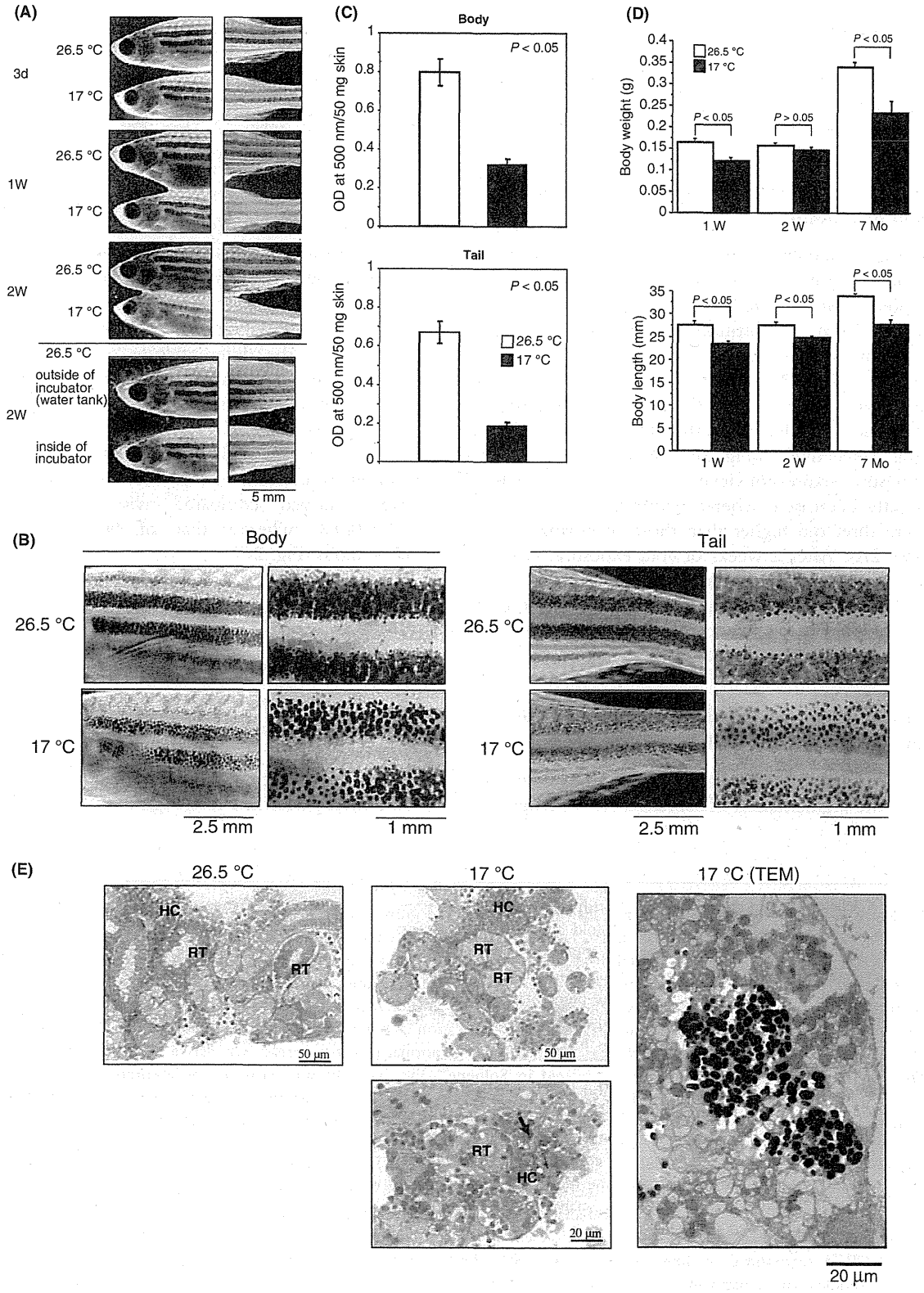

(TEM) were captured. As shown in Fig. 1E (right panel) and Fig. S2 in Supporting Information, abnormal melanophores are not similar to macrophage in KM, implying that they were not melanin-containing macrophages.

Expression of *csdc2*, *hspa8* and *ef1a* genes in the skin of zebrafish

We next examined whether cold exposure altered the expression of genes encoding cold- and heat-shock proteins, such as *csdc2* and *hspa8*, and elongation factor 1a (*ef1a*), a constitutive gene (Tang *et al.* 2007). Zebrafish were sampled at day 3, 1 and 2 weeks of cold exposure. On day 3, expression levels of *csdc2* and *hspa8* genes in the skin of cold zebrafish were 2.2- and 1.5-fold higher than those of normal zebrafish, respectively (Fig. 2A). After 1 week of cold exposure, expression levels of *csdc2* in cold zebrafish slightly decreased, whereas expression levels of *hspa8* were threefold higher than those of normal zebrafish (Fig. 2A). After 2 weeks of cold exposure, expression levels of both *csdc2* and *hspa8* were not changed. Cold exposure did not alter the expression of *elfa* at all time points, suggesting that cold exposure mainly modulated the expression of *csdc2* and *hspa8*.

Up-regulation of *pmch* and down-regulation of *tyr* and *dct* in cold zebrafish

To understand further how cold exposure down-regulates the pigmentation of zebrafish, we investigated the expression levels of several genes known to be involved in pigmentation. In the brains of cold zebrafish, expression levels of *pomca*, which is involved in melanosome dispersion, were increased at week 1 and then decreased at week 2 (Fig. 2B). *Pmch*, which was involved in melanosome aggregation, remained unchanged at week 1, but increased at week 2 (Fig. 2B). Expression levels of *tyr* and *dct*, which are involved in melanin synthesis, were also investigated. *Tyr* expression was decreased at weeks 1 and 2 of cold exposure, whereas *dct* was decreased at week 1 and then recovered to normal levels at week 2 (Fig. 2B).

We then investigated the expression of genes involved in the differentiation of melanoblasts into melanocytes. *Mitfa*, *kita* and *kitlga* have been identified as indicators for melanocyte differentiation during fin regeneration (Rawls & Johnson 2000). Two weeks after cold exposure, expression levels of *mitfa* and *kita* in the skin of cold zebrafish were not significantly altered compared with normal zebrafish ($P > 0.05$), whereas that of *kitlga* was increased ($P < 0.05$) (Fig. 2C).

Cold exposure reduces the number of melanophores

Our results of morphological observation, melanin content and gene expression enabled us to suggest that the down-regulation of pigmentation in cold zebrafish was caused by (i) down-regulation of melanin synthesis and/or (ii) decrease in the number of melanophores. We then performed histological analyses of skin sam-

Figure 1 Effects of cold exposure on zebrafish pigmentation and growth. (A) Gross appearances of normal and cold zebrafish and their background adaptation. Normal and cold zebrafish were maintained at 26.5 or 17 °C inside of incubator for 3 days (d), 1 week (W) and 2 W. The cold zebrafish appeared pale and depigmented. The degree of depigmentation correlated with the length of cold exposure. In background adaptation (lower panel), zebrafish were maintained at 26.5 °C in the incubator with appropriate light cycle. Two weeks later, the pigmentation of control zebrafish inside of incubator became slightly pale compared with zebrafish maintaining in water tank. (B) Higher magnification of pigment stripes on the body and tail. At 2 W, melanophores of cold zebrafish appeared as spots, whereas melanophores of normal zebrafish spread over larger areas. (C) Melanin content in zebrafish skin. The zebrafish skin was solubilized in Soluene®-350. Melanin was measured by absorption at 500 nm. The bar graphs show the means and standard deviation of optical density per 50 mg of zebrafish skin from three zebrafish per group. The Student's *t*-test was used for statistical analysis. (D) Effects of cold exposure on body weight and size of zebrafish. Cold exposure reduced the growth of zebrafish. Two-month-old zebrafish were maintained in water at 26.5 or 17 °C for 1 W, 2 W and 7 months (Mo). Body weight and length of cold zebrafish were significantly lower than those of normal zebrafish (upper and lower panels, respectively). The bar graphs show the means and standard deviations of body weight and length from 6 to 7 zebrafish per group. Student's *t*-test was used for statistical analysis. (E) Histology of kidney marrow (KM). KM was stained with Toluidine Blue O (left and middle) and observed by transmission electron microscopy (TEM) (right). In 26.5 °C water, there are normal renal tubules (RT) surrounded by hematopoietic cells (HC) (left). Cold zebrafish kept at 17 °C for 7 Mo exhibit abnormal RTs (upper middle). Black pigment-producing cells (lower middle, arrow) were observed only in cold zebrafish. TEM image shows melanin-containing granules in the KM of cold zebrafish (right).

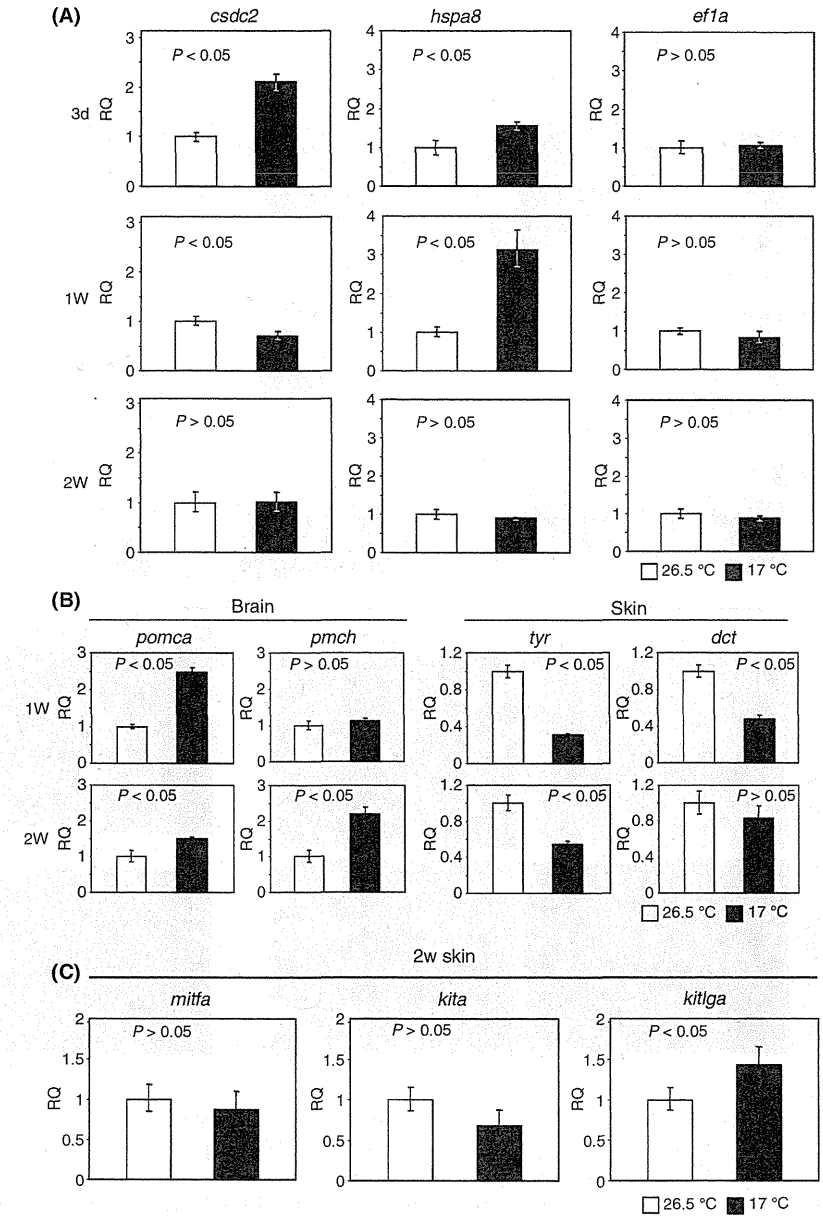

Figure 2 Expression levels of genes in normal and cold zebrafish (white and black bars, respectively). Levels of gene expression between normal and cold zebrafish were compared as relative quantities (RQ) on the *Y*-axis. (A) Expression levels of cold- and heat-shock protein genes, *csdc2* and *hspa8*, and a constitutively expressed gene, *ef1a*. Levels of *csdc2* and *hspa8* increased after 3 days (3 d) and 1 week (1 W) of cold exposure, whereas levels of *ef1a* were not changed. (B) Expression levels of genes involved in melanosome distribution, *pmoca* and *pmch*, and melanin synthesis, *tyr* and *dct*. In the brain of cold zebrafish, expression levels of *pmoca* increased at 1 W and slightly did at 2 W. Expression levels of *pmch* remained unchanged at 1 W, but increased at 2 W. In the skin, expression levels of *tyr* decreased both at 1 W and at 2 W, whereas *dct* decreased at 1 W and then recovered to normal levels. (C) Expression of genes involved in melanophore differentiation, *mitfa*, *kita* and *kitlga*, at the second week of cold exposure. Expression levels of *mitfa* and *kita* in cold zebrafish were not significantly different from normal zebrafish, whereas that of *kitlga* slightly was increased (~1.5-fold of normal zebrafish).

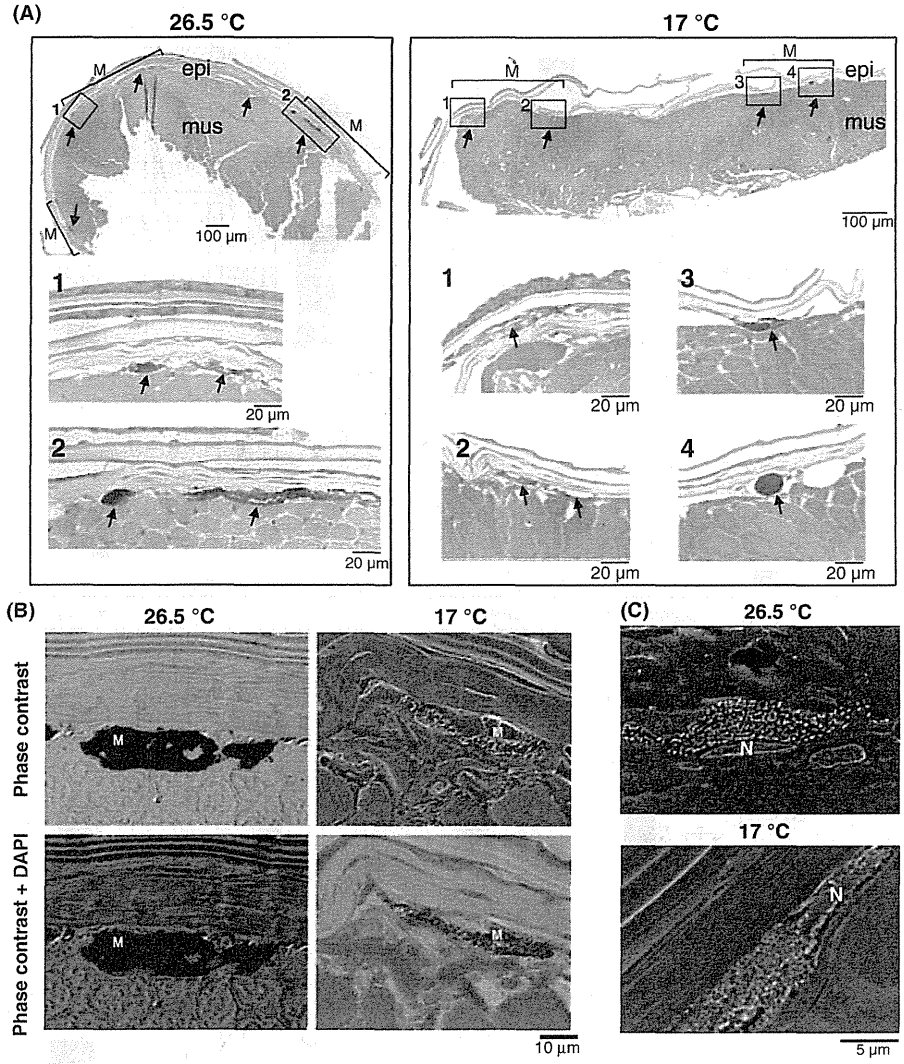

Figure 3 Histology of zebrafish skin. (A) Toluidine Blue O-stained zebrafish skin. Representative cross-sections of normal (26.5 °C) and cold (17 °C) zebrafish are shown. At lower magnification (upper panels), the number of melanophores (arrows) decreased in cold zebrafish. A series of melanophores (M) was localized between epidermis (epi) and muscle (mus) layers and named as melanophore band. The length of melanophore band in cold zebrafish (17 °C) was shorter than that of normal zebrafish (26.5 °C). At higher magnification (lower panels), the number of melanophores (arrows) decreased in melanophore bands of cold zebrafish compared with normal zebrafish. Lower panels are magnified view of boxes in upper panels. (B) Distribution of melanosomes in melanophores (M). Melanosomes were equally distributed in the cytoplasm of both normal and cold zebrafish. Nucleuses of melanophores were stained with DAPI and are located at the edge of cells (red arrows). There was no aggregation of melanosomes close to nucleus. (C) Images of scanning electron microscopy showed size, structure and distribution of melanosomes surrounding nucleus (N). There was no significant difference between normal and cold zebrafish.

ples using Toluidine Blue O staining and electron microscopy. At lower magnification (Fig. 3A, upper panels), we could observe a series of melanophores (arrows in upper panels of Fig. 3A) as if melanophores composed a band. The length of melanophore band in cold zebrafish (17 °C) was shorter than that of normal zebrafish (26.5 °C). When we examined a series of sections (results not shown), this observation was reproducible. At higher magnification, the number of melanophores decreased in the melanophore bands of cold zebrafish compared with normal zebrafish (Fig. 3A, lower panels). Taken together, it is likely that

the number of melanophores decreased in cold zebrafish. To investigate the distribution of melanosome in melanophores, we stained skin with DAPI that visualized nucleus. Melanosomes were equally distributed in the cytoplasm of both normal and cold zebrafish (Fig. 3B). There was no aggregation of melanosome close to nucleus (Red arrows in Fig. 3B). To quantify melanosome further, we performed scanning electron microscopy (SEM). Size and structure of melanosome in cold zebrafish were similar to normal zebrafish (Fig. 3C and Fig. S3 in Supporting Information). Taken together, cold exposure down-regulated adult zebrafish pigmentation through decreasing the number of pigmented melanophores.

Discussion

We have developed a novel model for pigmentation research. We show that adult zebrafish maintained at 17 °C water undergo depigmentation by decrease in pigmented melanophores. Overall melanin content in skin decreased without alteration in melanosome distribution in cold zebrafish. Pigment of adult zebrafish is composed of xanthophores, reflective iridophores and melanophores or melanocytes. Melanophore differentiation has been extensively studied during fin regeneration, and markers have been well described: *mitfa* for melanoblasts, *kita* for melanocytes and *tyr* and *dct* for pigmented melanophores (Rawls & Johnson 2000). In combination with these marker genes, we could evaluate melanophore differentiation and pigmentation. Expression levels of *mitfa* and *kita* genes remained unchanged, whereas that of *kitlga* was increased. It implies that melanophore differentiation was not altered and the increased expression of *kitlga* in cold zebrafish was because of a compensation mechanism. Although depigmentation in cold zebrafish was associated with *tyr* and *dct* down-regulation, decrease in the melanin-synthesizing enzymes does not certify the decrease in melanin because the activity of degradation enzyme might be down-regulated at low temperature. Gene expression of *try* and *dct* is identified in melanophores (Rawls & Johnson 2000; White & Zon 2008). The decrease in the number of melanophores might cause *tyr* and *dct* down-regulation in cold zebrafish.

Zebrafish have adaptation mechanisms that allow them to change the color of their pigment stripes within 24 h after background exposure (Logan *et al.* 2006); their pigmentation becomes lighter when exposed to white backgrounds and darker when exposed to black backgrounds. However, it is unlikely that the reduced pigmentation seen in cold zebrafish was because of background adaptation, because (i) we observed slight difference in pigmentation in zebrafish that were maintained inside or outside of the incubator and (ii) depigmentation occurred after 3 days of cold exposure, and not within 24 h (results not shown). This adaptation is caused by complex mechanisms existing in the endocrine and/or nervous systems (Fujii 2000). Melanosome aggregation in melanophores is also controlled by sympathetic neurons (Iwashita *et al.* 2006). Although gene expression of *pomca* and *pmch* encoding pro-hormones of melanocyte-stimulating hormone (MSC) and melanin-concentrating hormone (MCH), respectively, was up-regulated in cold zebrafish, there was no alteration in melanosome distribution in cold zebrafish, implying that sympathetic nervous system adjusted the melanosome distribution in cold zebrafish. It will be further necessary to investigate the involvement of nervous system in the future. Low temperatures down-regulate many physiologic processes (Sonna *et al.* 2002), but fish have compensatory mechanisms that allow adaptive survival in low temperatures (Cossins *et al.* 2002; Schwarzbaum *et al.* 1992a,b). In Arctic fish, it has been reported that the activity levels of ion pumps and Na^+/K^+-ATPases in the kidney are increased to balance the altered ion concentrations and body fluid pH caused by temperature acclimation (Schwarzbaum *et al.* 1992a,b). The abnormal renal tubules and melanophores in the KM of cold zebrafish might be due to similar adaptation mechanisms.

Cold- and heat-shock proteins are thought to play important roles in adaptation to cold exposure in vertebrates (Ali *et al.* 2003; Al-Fageeh & Smales 2006). Although their functions are not fully understood, it has been suggested that cold-shock proteins bind mRNA to regulate transcription and translation. We analyzed the expression levels of *csdc2* and *hspa8* genes in the skin of zebrafish to investigate the molecular relationships between cold exposure and pigmentation. Csdc2 contains an S1-like CSD, which is conserved in the cold-shock protein family proteins, and Hspa8 is one of the heat-shock protein 70 family proteins. It was reported that, under cold shock, Hspa8 is up-regulated in carp (Ali *et al.* 2003). In this study, gene expression of both *csdc2* and *hspa8* was up-regulated in the skin of cold zebrafish compared with normal zebrafish. This result implies that Csdc2 and Hspa8 directly or indirectly have a role in regulating pigmentation. Further investigation into this relationship is warranted.

In humans, abnormal melanin synthesis results in diseases such as hypopigmentation in albinism and hyperpigmentation in melasma, postinflammatory melanoderma and solar lentigines (Ni-Komatsu & Orlow 2007). Novel genes involved in the regulation of melanin synthesis can be potentially identified with this cold zebrafish model. Moreover, *dct* is associated with cisplatin-resistant malignant melanoma (Miller & Mihm 2006; Pak *et al.* 2004). However, the relationship between *dct* and melanoma biology still remains to be elucidated (White & Zon 2008). Further investigations to understand better the molecular mechanisms involved in the formation of malignant melanomas are warranted. Our cold zebrafish model may provide important insights into melanoma biology in the future.

Experimental procedures

Maintenance of zebrafish

Zebrafish (*Danio rerio*, India strain) born from the same parent were housed in tanks with recirculating dechlorinated tap water at 26.5 °C (room temperature) for 2 months. Two-month-old zebrafish were then separated into two groups: the first group was grown in 17 °C water inside an incubator for 3 days, 1, 2 weeks and 7 months and the second group was continuously maintained at 26.5 °C. Food, water and light cycles for both groups were controlled under the same conditions. To assess the presence of background adaptation in the incubators, one set of zebrafish was maintained inside and one set outside of the incubators in 26.5 °C water for 2 weeks, under the same conditions as mentioned earlier. The inside of incubator was covered by metal sheet.

Measurement of melanin content in zebrafish skin by spectrophotometer

Melanin content was measured following the method of Hultman & Johnson (2010) with a little modification. Zebrafish skin at body and tail was separately dissected out and weighted. Soluene®-350 (PerkinElmer, MA, USA) was added at a ratio 250 μL/50 mg skin and was heated at 95 °C for 1 h. After cooling, samples were centrifuged. Melanin in supernatant was assayed by absorption at 500 nm on a Nanodrop spectrophotometer (Thermo Fisher Scientific Inc.).

Growth measurement

Body weight and length were measured before killing the adult zebrafish to observe the effects of cold exposure on growth. Phenotypes were observed under a back-lit microscope (Olympus SZX16, Tokyo, Japan), and high-resolution

Table 1 Primer sets for zebrafish genes that are involved in pigmentation. Primers were designed using PRIMER EXPRESS® software version 3.0

Genes		Sequence (5′ → 3′)	Size (bp)	Reference sequences
bactin2	F	TGCTCCCCGAGCTGTCTT	64	NM_181601.3
	R	ACCAACCATGACACCCTGATG		
csdc2	F	CACACACCTCTCTCGCTTTCAT	100	NM_001002690.1
	R	TTGGCAGTGGACTCAGAGGTT		
dct	F	TTCACTCTCTGAGTCCGGAAGAG	100	NM_131555.1
	R	CAGTGCTGTGTGGCGATCAT		
ef1a	F	TCTACAAATGCGGTGGAATCG	100	NM_131263.1
	R	TCCAACACCCAGGCGTACTT		
hspa8	F	GATCGGCAGGAGGTTCGA	100	NM_001110403
	R	TTCCACTGCAACTTTTGGCTTT		
kita	F	ATCCTGCTCCACCTCAAATG	112	NM_131053.1
	R	GAGTAATGGGCTCCGTCAGA		
kitlga	F	GCCTGATGACCCCGAAAAA	100	XM_001922513.1
	R	CAAAACCACCACTGCGATTG		
mitfa	F	ATTCTTGGGTTCATGGATGCA	100	NM_130923.1
	R	CAGCTGGAGGAAGAGCATGAT		
pmch	F	TGGATGAGCAACGTAACGTAGAA	100	FJ392644.1
	R	TGCCAGCAGGGCCTGTATAC		
pomca	F	GAAGAGGAATCCGCCGAAA	98	NM_181438.3
	R	CCAGTGGGTTTAAAGGCATCTC		
tyr	F	GGTGCCCTTCATCCCTCTCT	100	NM_131013.1
	R	AAACCGCTGACCTGGATCCT		

TIFF images were acquired using an Olympus DP71 camera (Tokyo, Japan) attached to the microscope.

Dissection of zebrafish

Dissections were performed as previously described (Ivanovski *et al.* 2009). Briefly, adult zebrafish were anesthetized with 0.02% tricaine. Under the Olympus SZX16 (Tokyo, Japan), the superficial layers (outer epidermis and the underlying dermis) were carefully dissected out using two microforceps with 0.3-mm tips (World Precision Instruments, Sarasota, FL) and placed in RNA*later* (Life Technologies, Carlsbad, CA, USA). Muscles were dissected along the body. KMs, which are dark red–colored tissue with black dots and flanked by vertebral bones (Ivanovski *et al.* 2009), and brains were also dissected out and placed in RNA*later* (Life Technologies).

Real-time PCR

RNA extractions from skin, brain and KM were carried out using RiboPure™ kits (Life Technology), and mRNA was reverse-transcribed using High-Capacity RNA-to-cDNA kits (Life Technology). cDNA quality was evaluated by amplifying *bactin2*. Thirty thermal cycles were performed as follows: first denaturation at 95 °C for 10 s, annealing at 60 °C for 20 s and extension at 72 °C for 20 s. Gene expression levels were measured by StepOnePlus™ real-time PCR (Life Technology) using Fast SYBR® Green Master Mix. Primers were designed using PRIMER EXPRESS® software version 3.0 (Life Technology) and are shown in Table 1.

Histology of KM

Kidney marrows were fixed in 4% paraformaldehyde and 0.25% glutaraldehyde overnight. After three washes in PBS and once in 20% sucrose in PBS, the zebrafish were embedded into O.C.T. compound (SAKURA Tissue-Tek®; Torrance, CA, USA) and snap-frozen in liquid nitrogen before storage in −80 °C. For cryosections, the embedded zebrafish were cut cross-section into 10-μm slices and stained with Toluidine Blue O (Wako Pure Chemical Industries Ltd., Osaka, Japan). Stained cryosections were magnified at ×10, and the images were captured on an Olympus CKX41 microscope (Tokyo, Japan).

Histology of skin

Zebrafish were fixed in 0.1% paraformaldehyde and 4% glutaraldehyde overnight. After three washes in PBS, zebrafish were fixed in 2% OsO_4 at 4 °C for 2 h. Samples were dehydrated in 50%, 75%, 85% and 100% acetone for 10 min each. Dehydrated zebrafish were embedded in Technovit 8100 (Heraeus Kulzer GmbH, Hanau, German). The embedded zebrafish were cut cross-section into 3–4 μm by ultramicrotome (semi-thin) and stained with Toluidine Blue O (Wako Pure Chemical Industries Ltd.) or DAPI.

Electron microscopy

Scanning electron microscopy and TEM were performed as described by previously (Yahiro & Nagato 2005) with modification. For SEM, the embedded zebrafish were cut cross-section as semi-thin on Si-Chips. Ion etching was performed by hard mode 3 min × 2 times. Then, ion bombarder was performed by soft mode 3 min × 1 time. Tissues were coated with osmium (2.5 nm) and observed. For TEM, KMs were embedded in Epon 812 (Shell Chemical, San Francisco, CA, USA) and cut cross-section into 90 nm (ultrathin). Tissues were stained with uranyl acetate and lead and observed.

Acknowledgements

The authors acknowledge grant support from the Special Coordination Funds for Promoting Science and Technology and the Nagao Memorial Fund. Kasem Kulkeaw is a scholar of the Ajinomoto Scholarship Foundation, and Ognen Ivanovski is a research fellow of the Inoue Scientific Foundation. We also thank Drs. Sumio Isogai for many helpful discussions, and Dr Tomoko Inoue (Yokoo) and Mr Tatsuya Sasaki for their technical assistance.

References

Al-Fageeh, M.B. & Smales, C.M. (2006) Control and regulation of the cellular responses to cold shock: the responses in yeast and mammalian systems. *Biochem. J.* **397**, 247–259.

Ali, K.S., Dorgai, L., Abraham, M. & Hermesz, E. (2003) Tissue- and stressor-specific differential expression of two hsc70 genes in carp. *Biochem. Biophys. Res. Commun.* **307**, 503–509.

Cossins, A.R., Murray, P.A., Gracey, A.Y., Logue, J., Polley, S., Caddick, M., Brooks, S., Postle, T. & Maclean, N. (2002) The role of desaturases in cold-inducing lipid restructuring. *Biochem. Soc. Trans.* **30**, 1082–1086.

Fujii, R. (2000) The regulation of motile activity in fish chromatophores. *Pigment Cell Res.* **13**, 300–319.

Hultman, K.A. & Johnson, S.L. (2010) Differential contribution of direct-developing and stem cell-derived melanocytes to the zebrafish larval pigment pattern. *Dev. Biol.* **337**, 425–431.

Ivanovski, O., Kulkeaw, K., Nakagawa, M., Sasaki, T., Mizuochi, C., Horio, Y., Ishitani, T. & Sugiyama, D. (2009) Characterization of kidney marrow in zebrafish (*Danio rerio*) by using a new surgical technique. *Prilozi* **30**, 71–80.

Iwashita, M., Watanabe, M., Ishii, M., Chen, T., Johnson, S.L., Kurachi, Y., Okada, N. & Kondo, S. (2006) Pigment pattern in jaguar/obelix zebrafish is caused by a Kir7.1 mutation: implications for the regulation of melanosome movement. *PLoS Genet.* **24**, e197.

Johnson, S.L. & Weston, J.A. (1995) Temperature-sensitive mutations that cause stage specific defects in zebrafish fin regeneration. *Genetics* **141**, 1588–1595.

Kelsh, R.N. & Eisen, J.S. (2000) The zebrafish *colourless* gene regulates development of non-ectomesenchymal neural crest derivatives. *Development* **127**, 515–525.

Kulkeaw, K., Ishitani, T., Kanemaru, T., Fucharoen, S. & Sugiyama, D. (2010) Cold exposure down-regulates zebrafish hematopoiesis. *Biochem. Biophys. Res. Commun.* **394**, 859–864.

Lister, J.A., Robertson, C.P., Lepage, T., Johnson, S.L. & Raible, D.W. (1999) Nacre encodes a zebrafish microphthalmia-related protein that regulates neural-crest-derived pigment cell fate. *Development* **126**, 3757–3767.

Logan, D.W., Burn, S.F. & Jackson, J. (2006) Regulation of pigmentation in zebrafish melanophores. *Pigment Cell Res.* **19**, 206–213.

Malek, R.L., Sajadi, H., Abraham, J., Grundy, M.A. & Gerhard, G.S. (2004) The effects of temperature reduction on gene expression and oxidative stress in skeletal muscle from adult zebrafish. *Comp. Biochem. Physiol. C Toxicol. Pharmacol.* **138**, 363–373.

Miller, A.J. & Mihm, M.C. Jr (2006) Melanoma. *N. Engl. J. Med.* **355**, 51–65.

Ni-Komatsu, L. & Orlow, S.J. (2007) Identification of novel pigmentation modulators by chemical genetic screening. *J. Invest. Dermatol.* **127**, 1585–1592.

Pak, B.J., Lee, J., Thai, B.L., Fuchs, S.Y., Shaked, Y., Ronai, Z., Kerbel, R.S. & Ben-David, Y. (2004) Radiation resistance of human melanoma analysed by retroviral insertional mutagenesis reveals a possible role for dopachrome tautomerase. *Oncogene* **23**, 30–38.

Parichy, D.M., Ransom, D.G., Paw, B., Zon, L.I. & Johnson, S.L. (2000) An ortholog of the *kit*-related gene *fms* is required for development of neural crest-derived xanthophores and a subpopulation of adult melanocytes in the zebrafish *Danio rerio*. *Development* **127**, 3031–3044.

Parichy, D.M., Rawls, J.F., Pratt, S.J., Whitfield, T.T. & Johnson, S.L. (1999) Zebrafish sparse corresponds to an orthologue of c-kit and is required for the morphogenesis of a subpopulation of melanocytes, but is not essential for hematopoiesis or primordial germ cell development. *Development* **126**, 3425–3436.

Rawls, J.F. & Johnson, S.L. (2000) Zebrafish kit mutation reveals primary and secondary regulation of melanocyte development during fin stripe regeneration. *Development* **127**, 3715–3724.

Rawls, J.F. & Johnson, S.L. (2001) Requirements for the kit receptor tyrosine kinase during regeneration of zebrafish fin melanocytes. *Development* **128**, 1943–1949.

Schwarzbaum, P.J., Niederstätter, H. & Wieser, W. (1992a) Effects of temperature on the (Na^++K^+)-ATPase and oxygen consumption in hepatocytes of two species of freshwater fish, Roach (*Rutilus rutilus*) and Brook Trout (*Salvelinus fontinalis*). *Physiol. Zool.* **65**, 699–711.

Schwarzbaum, P.J., Wieser, W. & Cossins, A.R. (1992b) Species-specific responses of membranes and the Na^++K^+ pump to temperature change in the kidney of two species of freshwater fish, roach (*Rutulis rutulis*) and Arctic char (*Salvelinus alpinus*). *Physiol. Zool.* **65**, 17–34.

Sonna, L.A., Fujita, J., Gaffin, S.L. & Lilly, C.M. (2002) Invited review: effects of heat and cold stress on mammalian gene expression. *J. Appl. Physiol.* **92**, 1725–1742.

Tang, R., Dodd, A., Lai, D., McNabb, W.C. & Love, D.R. (2007) Validation of zebrafish (*Danio rerio*) reference genes for quantitative real-time RT-PCR normalization. *Acta Biochim. Biophys. Sin. (Shanghai)* **39**, 384–390.

White, R.M. & Zon, L.I. (2008) Melanocyte in development, regeneration, and cancer. *Cell Stem Cell* **3**, 242–252.

Yahiro, J. & Nagato, T. (2005) Application of ion etching to immunoscanning electron microscopy. *Microsc. Res. Tech.* **67**, 240–247.

Received: 26 July 2010
Accepted: 26 December 2010

Supporting Information/Supplementary material

The following Supporting Information can be found in the online version of the article:

Figure S1 Gross appearance of cold zebrafish before and after cold exposure.

Figure S2 Electron microscopic observation of zebrafish kidney marrow.

Figure S3 Electron microscopic observation of melanophore in skin of cold zebrafish.

Additional Supporting Information may be found in the online version of this article.

Please note: Wiley-Blackwell are not responsible for the content or functionality of any supporting materials supplied by the authors. Any queries (other than missing material) should be directed to the corresponding author for the article.

Stem Cell Rev and Rep (2011) 7:43–52
DOI 10.1007/s12015-010-9140-7

APOA-1 is a Novel Marker of Erythroid Cell Maturation from Hematopoietic Stem Cells in Mice and Humans

Tomoko Inoue · Daisuke Sugiyama · Ryo Kurita · Tatsuo Oikawa · Kasem Kulkeaw · Hirotaka Kawano · Yoshie Miura · Michiyo Okada · Youko Suehiro · Atsushi Takahashi · Tomotoshi Marumoto · Hiroyuki Inoue · Norio Komatsu · Kenzaburo Tani

Published online: 8 April 2010

Abstract The mechanism that regulates the terminal maturation of hematopoietic stem cells into erythroid cells is poorly understood. Therefore, identifying genes and surface markers that are restricted to specific stages of erythroid maturation will further our understanding of erythropoiesis. To identify genes expressed at discrete stages of erythroid development, we screened for genes that contributed to the proliferation and maturation of erythropoietin (EPO)-dependent UT-7/EPO cells. After transducing erythroid cells with a human fetal liver (FL)-derived lentiviral cDNA library and culturing the cells in the absence of EPO, we identified 17 candidate genes that supported erythroid colony formation. In addition, the mouse homologues of these candidate genes were identified and their expression was examined in E12.5 erythroid populations by qRT-PCR. The expression of candidate erythroid marker was also assessed at the protein level by immunohistochemistry and ELISA. Our study demonstrated that expression of the *Apoa-1* gene, an apolipoprotein family member, significantly increased as hematopoietic

Electronic supplementary material The online version of this article (doi:10.1007/s12015-010-9140-7) contains supplementary material, which is available to authorized users.

T. Inoue · R. Kurita · T. Oikawa · H. Kawano · Y. Miura · M. Okada · Y. Suehiro · A. Takahashi · T. Marumoto · H. Inoue · K. Tani (✉)
Department of Molecular Genetics,
Medical Institute of Bioregulation, Kyushu University,
3-1-1, Maidashi, Higashi-ku,
Fukuoka 812-8582, Japan
e-mail: taniken@bioreg.kyushu-u.ac.jp

T. Inoue
e-mail: yokotomo@bioreg.kyushu-u.ac.jp

R. Kurita
e-mail: k-ryo@brc.riken.jp

T. Oikawa
e-mail: oitatsullo@yahoo.co.jp

H. Kawano
e-mail: kawano@bioreg.kyushu-u.ac.jp

Y. Miura
e-mail: ymiura@bioreg.kyushu-u.ac.jp

M. Okada
e-mail: okadatch@bioreg.kyushu-u.ac.jp

Y. Suehiro
e-mail: suehiro@sentan.med.kyushu-u.ac.jp

A. Takahashi
e-mail: atsushi@sentan.med.kyushu-u.ac.jp

T. Marumoto
e-mail: marumoto@sentan.med.kyushu-u.ac.jp

H. Inoue
e-mail: hinoue@bioreg.kyushu-u.ac.jp

D. Sugiyama
Faculty of Medical Sciences, Department of Hematopoietic Stem Cells, SSP Stem Cell Unit, Kyushu University,
3-1-1, Maidashi, Higashi-ku,
Fukuoka 812-8582, Japan
e-mail: sugiyama@hsc.med.kyushu-u.ac.jp

K. Kulkeaw
Faculty of Medical Sciences, Department of Hematopoietic Stem Cells, SSP Stem Cell Unit, Kyushu University,
3-1-1, Maidashi, Higashi-ku,
Fukuoka 812-8582, Japan
e-mail: kkulkeaw@yahoo.com

N. Komatsu
Department of Transfusion Medicine and Stem Cell Regulation,
Juntendo University School of Medicine,
2-1-1, Hongo, Bunkyo-ku,
Tokyo 113-8431, Japan
e-mail: komatsun@juntendo.ac.jp

stem cells differentiated into mature erythroid cells in the mouse FL. The Apoa-1 protein was more abundant in mature erythroid cells than hematopoietic stem and progenitor cells in the mouse FL by ELISA. Moreover, *APOA-1* gene expression was detected in mature erythroid cells from human peripheral blood. We conclude that APOA-1 is a novel marker of the terminal erythroid maturation of hematopoietic stem cells in both mice and humans.

Keywords APOA-1 · Erythroid cell maturation · Fetal liver erythropoiesis · Library screening · Lentiviral cDNA library

Introduction

Hematopoiesis is the process in which pluripotent hematopoietic stem cells (HSCs) are generated, differentiated into specific progenitors, and ultimately matured into a variety of blood cell types (erythrocytes, megakaryocytes, lymphocytes, neutrophils, and macrophages) [1]. During embryonic development, HSCs emerge in the aorta-gonad-mesonephros (AGM) region and expand first in the fetal liver (FL) and then in the bone marrow (BM) [2–5]. Among these hematopoietic organs, the FL is a site of both HSC expansion and active erythropoiesis [6]. Erythropoiesis is the process by which a vast number of enucleated red blood cells (RBCs) are produced from hematopoietic stem cells (HSC) [7]. However, the molecular mechanisms underlying erythropoiesis have not been fully elucidated, largely because there are only a few molecular markers of terminal erythroid maturation in both mice and humans. To address this issue, we focused on the events that regulate the terminal erythropoiesis of HSCs to mature erythroid cells in order to identify novel markers of mature erythrocytes.

A previous study established a mouse embryonic (ES) cell-derived erythroid progenitor (MEDEP) cell line [8]. Although erythroblasts expressing the erythroid maturation marker Ter119 [9] (a protein that molecularly resembles glycophorin) can be generated from ES/iPS-derived MEDEP cells, most of these cells remained nucleated, indicating that they have failed to complete terminal maturation. Ter119 antigen is currently the only erythroid-specific marker in mice. However, Ter119 is expressed at many maturation stages, from erythroblasts to mature, circulating erythrocytes. Therefore, additional markers for mature erythrocytes are needed. Numerous attempts at generating vast quantities of enucleated erythrocytes have failed to efficiently give rise to fully functional erythrocytes in vitro. This may in part be due to the gaps in our understanding of the mechanisms that regulate erythropoiesis.

The cytokine erythropoietin (EPO) plays important roles in erythropoiesis by regulating erythroid cell differentiation, maturation, proliferation, and survival. Erythroid cells are highly dependent on EPO during early differentiation and maturation but lose this dependency and express lower levels of the erythropoietin receptor (EPOR) as they mature [10]. We hypothesized that EPO-independent signaling plays an important role in the terminal stages of erythropoiesis.

We previously established a system in which specific lentiviral gene transduction induced hematopoiesis from embryonic stem cells of a nonhuman primate common marmoset in the absence of bone marrow stromal cells [11]. In addition, we constructed a high-performance human fetal liver (FL)-derived cDNA lentiviral library as a tool to facilitate the discovery of novel genes that are involved in the expansion of HSCs, erythropoiesis and/or liver development [12]. During embryogenesis, the FL is the major site of hematopoiesis, particularly erythropoiesis. Therefore, the FL-derived cDNA lentiviral library that we constructed contains many genes that are involved in the differentiation and maturation of these lineages. The goal of this study was to identify novel genes that are involved in or expressed during EPO-independent terminal erythroid maturation. We identified APOA-1 as a novel marker of the maturation of hematopoietic stem cells into mature erythroid cells.

Materials and Methods

Cells

UT-7/EPO cells [13] (kindly provided by Dr. Komatsu) are an EPO-dependent cell line that was established from the bone marrow of a patient with acute megakaryoblastic leukemia. This cell line was cultured in Iscove's modified Dulbecco's medium (IMDM) supplemented with 10% fetal bovine serum (FBS) and 1 U/mL human recombinant EPO (R&D Systems, Minneapolis, MN) at 37°C in 5% CO_2.

Lentivirus Production

The previously generated human fetal liver-derived Entry cDNA library [12] was used in this study. Briefly, 34 μg ($1–2\times10^5$ cDNA clones) of the library was mixed with 20 μg of pCAG-HIVg/p and 20 μg of pCMV-VSVG-RSV-Rev as the packaging plasmids in 3.5 ml of FBS-free DMEM, and then 370 μl of 1 mg/ml polyethylenimine (PEI) was added to the mixture. After a 30-min incubation, the DNA/PEI complexes were dropped onto semi-

confluent 293 T cells in a T175 flask containing Opti-MEM medium and then incubated for 3 h. Next, these cells were cultured in DMEM containing 10% FBS. Virus-containing supernatants were harvested 4 days post transduction and concentrated by centrifugation (9,000 rpm, 6–8 h, 4°C). The virus pellet was resuspended in 1 ml of IMDM and used for overnight transduction of UT-7/EPO cells.

Transduction of the Lentiviral Library into UT-7/EPO Cells

UT-7/EPO cells were transduced with the viral cDNA library and cultured in methylcellulose semi-solid medium containing IMDM, 10% FBS, and P/S without EPO for one month. After this period, several colonies were harvested, and genomic DNA was isolated from each colony using the QIAamp DNA Micro Kit (Qiagen, Valencia, CA).

Genomic PCR and Sequence Analysis

The integrated cDNAs were PCR amplified using a forward primer (5′-TTCAGGTGTCGTGAACACGCTACCG-3′) and reverse primer (5′-CCTCGATGTTAACTCTAGAG GATCC-3′). The Expand Long Template PCR System (Roche, Basel, Switzerland) was used following the manufacturer's protocol. cDNAs that were cloned into the CSII-CMV-RfA vector were sequenced with the forward (5′-CAAGCCTCAGACAGTGG-3′) and reverse (5′-AGCG TATCCACATAGCG-3′) primers using a Big-Dye Terminator v3.1 Cycle sequencing kit (Applied Biosystems, Foster City, CA) and an ABI PRISM 3100 Genetic Analyzer (Applied Biosystems). The sequences were compared with the DNA database from the DNA Data Bank of Japan using BLAST.

Cell Culture and Sorting

The EPO-dependent UT-7/EPO cell line was established and cultured as previously reported [13]. C57BL6J mice and ICR mice were purchased from Nihon SLC. Twelve o'clock noon was considered to be 0.5 day postcoitum (dpc) for plugged mice. Fetal liver (FL) cells from a 12.5 dpc embryo were filtered through a 40 μM nylon mesh and washed with PBS. The cells were stained with a FITC-conjugated anti-mouse CD71 Ab (BD Biosciences), PE-conjugated anti-mouse Sca-1 Ab (BD Biosciences), APC-conjugated anti-mouse c-Kit Ab (BD Biosciences), PE-Cy7-conjugated anti-mouse CD45 Ab (eBioscience) and APC-Cy7-conjugated anti-mouse Ter119 Ab (eBioscience). The cells were sorted using a FACS Aria cell sorter (BDIS), and the data files were analyzed using FlowJo software (Tree Star, Inc.).

Human peripheral blood (PB) was obtained from healthy volunteers. The PB was stained with a FITC-conjugated anti-human CD45 Ab (eBioscience), PE-conjugated anti-GPA antibody (eBioscience) and APC-conjugated anti-human CD41 antibody (BD Bioscience). The cells were sorted using a FACS Aria cell sorter (BDIS), and the data files were analyzed using FlowJo software (Tree Star, Inc.).

All animal studies were approved by the Committee on Ethics in Animal Experiments of Kyushu University, and the human studies were approved by the Committee on Ethics in Human clinical samples of Kyushu University. All of these studies were performed following the guidelines of Kyushu University.

RNA Extraction and Real-time RT-PCR

Total RNA was isolated from FL cells of ICR embryos at 12.5 dpc or whole embryos at 10.5 dpc using the RNAqueous-4PCR kit (Ambion). Total RNA from human peripheral blood was isolated with the RiboPure Kit (Ambion). A high-capacity cDNA Archive kit (Applied Biosystems) was used to synthesize cDNA from RNA. The mRNA levels of various genes were analyzed by qRT-PCR using SYBR Green and gene-specific primers with the StepOnePlus real-time PCR system (Applied Biosystems). The mRNA level of each target gene was normalized to β-actin as an internal control.

Immunohistochemistry

Ter119-positive cells from 12.5 dpc FL cells were isolated by flow cytometry as described above. Cells were cytospun onto glass slides and air-dried. The cells were fixed in 1% PFA at room temperature (RT) for 10 min. Nonspecific binding was blocked by incubating the cells at RT for 30 min in a blocking solution containing 1% BSA and 0.05% Triton X-100 in PBS. The following antibodies were diluted in the blocking solution: rabbit anti-Apoa-1 (1:50, Santa Cruz Biotechnologies, Inc.). A donkey anti-rabbit IgG (H+L)-Alexa555 (1:250, Invitrogen) was used as secondary antibody and TOTO-3 (1:1500, Invitrogen) was added as a nuclear stain. Coverslips were mounted with fluorescent mounting medium (Dako), and the slides were examined using a confocal microscope (Olympus).

ELISA

c-Kit-positive cells and Ter119-positive cells were isolated by flow cytometry as described above. Proteins were extracted from the sorted cells using the Qproteome Mammalian Protein Preparation kit (Qiagen). To detect the Apoa-1 protein, a goat anti-Apoa-1 (0.8 μg/ml,

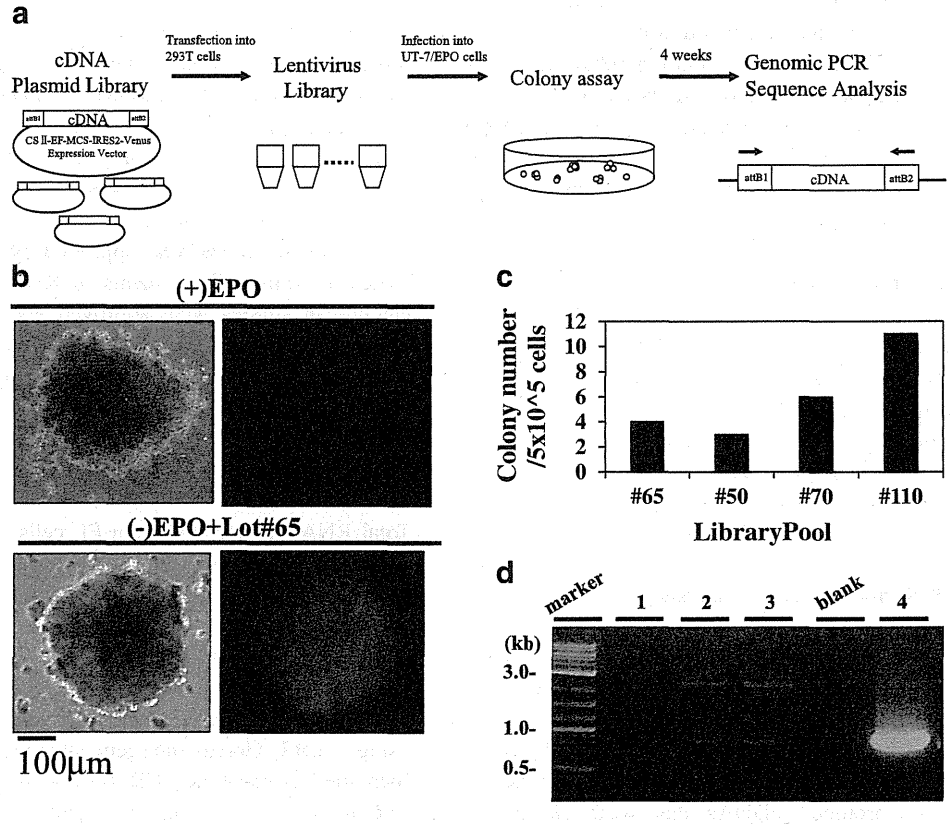

Fig. 1 Lentiviral human FL cDNA library screening in UT-7/EPO cells. **a** Strategy for identifying candidate EPO-independent regulators of erythropoiesis. Four pools (#65, #50, #70 and #110) of human FL-derived cDNA library were transfected into 293 T cells with helper plasmids to generate the lentiviral library. UT-7/EPO cells were transduced with these lentiviral library pools and then cultured in semisolid, EPO-deficient media for four weeks to positively select for clones that were able to form EPO-independent erythroid colonies. Finally, the cDNAs of the positive clones were sequenced to identify the transduced genes. **b** Erythroid colony assay. UT-7/EPO cells were transduced with the lentiviral pools (#65, #50, #70 and #110) and then transferred to semi-solid culture media. A representative colony derived from cells transduced with pool #65 is shown (Scale bar= 200 μm). A non-transduced colony was negative for Venus, while the lentiviral library-transduced colony was positive for Venus. **c** Colony number. A total of 22 colonies were obtained from UT-7/EPO cells that had been transduced with four lentiviral library pools and then analyzed by the colony formation assay. **d** Genomic PCR analysis. The inserted candidate genes were examined by genomic PCR using lentivirus insertion-specific primers. Lane 1: Untransduced UT-7/EPO cells (negative control), Lanes 2, 3: A colony derived from UT-7/EPO cells that had been transduced with lentiviral pool #65, Lane 4: GFP-transduced UT-7/EPO cells (positive control)

Rockland Immunochemicals) was used as a capture antibody, a rabbit anti-Apoa-1 (1:100, Santa Cruz Biotechnologies, Inc.,) was used as a detection antibody (primary antibody), and an anti-rabbit IgG-HRP (1:5000, Millipore) was used as the secondary antibody. Each antibody was captured onto 96-well immunoplates (Nunc) at 4°C for 16 h. Nonspecific binding was blocked by incubating the plate with 1% BSA/PBS for 2 h at RT. After the extracted proteins were added to the plate for 2 h at RT, the primary antibody was added for 1 h at RT, followed by the secondary antibody for 30 min at RT. The tetramethylbenzidine substrate was added to the wells for 30 min at RT, followed by a Stop Solution (R&D). The O.D. at 450 nm was measured using a Thermo Multiskan EX plate reader.

Results

Screening for Genes that Replace EPO/EPOR Signaling in UT-7/EPO Cells Using a Human FL Lentiviral Library

To identify novel genes that regulate erythroid cell maturation, we designed a strategy that monitored the ability of the EPO-dependent cell line, UT-7/EPO, to form erythropoietin (EPO)-independent colonies. Recently, we constructed a lentiviral human fetal liver (FL) cDNA library to search for novel genes that regulate hematopoiesis, including erythropoiesis [14]. Lentiviral cDNA library pools, which contained $1.32–1.98 \times 10^5$ cfu (colony forming units) per pool [14], were examined in this screen. We used the UT-7/EPO cell line, which is dependent upon EPO [13].

Table 1 Genes transduced in lentiviral-transduced erythroid colonies arising in the absence of Epo

Lentivirus pool #	Gene symbol	Discription
65	Angiotensinogen	AGT
	Estrogen receptor binding site associated antigen 9	EBAG9
50	B-cell CLL/lymphoma 2-like 1	BCL2-like 1
	Apolipoprotein A-1	APOA-1
70	ferritin heavy subunit	FHS
	3-phosphoinositide dependent protein kinase-1	PDPK1
	abl interactor 2	ABI-2
	Fibrinogen like 1	FGL1
	Apolipoprotein E	APOE
	Interferon induced transmembrane protein 2	1-8D
110	Asialoglycoprotein receptor 2	ASGR2
	Ferritin light chain	FLC
	Solute carrier family 27 (fatty acid transporter)	SLC27A2
	Ribosomal protein L10	RPL10
	Collagen type XVIII alpha 1	COL18A1
	Apolipoprotein J	APOJ
	Group-specific component	GC

When UT-7/EPO cells are transduced with genes in this lentiviral library that can functionally replace EPO/EPOR signaling, expression of these genes will result in colony formation in the absence of EPO (Fig. 1a). 293 T cells were transfected with four different lentiviral cDNA pools (#65, #50, #70 and #110). Subsequently, UT-7/EPO cells were transduced with these four different lentivirus library pools and cultured for four weeks in semi-solid media in the absence of EPO. Clones that acquired the ability to proliferate in the absence of EPO were identified and analyzed. Lentiviral-transduced cells were identified by Venus fluorescence that was encoded by the lentiviral vector. UT-7/EPO cells that were cultured in the absence of EPO failed to generate colonies, whereas these cells generated equal numbers of colonies when cultured in semi-solid media containing EPO (data not shown). When UT-7/EPO cells that had been transduced with the lentiviral library (6×10^5 cDNAs) were cultured in the absence of EPO, 22 EPO-independent colonies formed (Fig. 1b–c).

Next, to identify the cDNAs responsible for this EPO-independent proliferation, genomic DNA was isolated from each colony, and the integrated cDNAs were PCR amplified using lentivirus-specific primers (Fig. 1d). Agarose gel electrophoresis of the PCR products for each colony showed multiple bands of different sizes (Fig. 1d, lanes 2 and 3). This amplification was specific because untransduced UT-7/EPO cells did not yield any PCR products (lane 1), and a PCR product of the expected size was amplified from UT-7/EPO cells transduced with a lentivirus encoding green fluorescent protein (GFP) (lane 4).

Candidate Genes Identified from UT-7/EPO Cells Transduced with Human FL Lentiviral cDNA Library

The PCR products from the first round of screening were sequenced to identify the candidate genes that were expressed during erythropoiesis. Each pool contained a different number of inserted genes (Table 1). From the first screening, the following genes were identified as candidates that contributed to the growth of EPO-independent colonies; *FHS* and *FLC* encoding iron-binding proteins; the vitamin D-binding protein *GC*; the plasma protein receptor *ASGR2*; the vasoregulator *AGT*; estrogen-responsive protein *EBAG9*; the collagen *COL18A1*; the ribosomal protein *RPL10*; the kinase *PDPK1*; *ABI-2*, a kinase-binding protein; *APOA-1*, *APOE, APOJ* and *SLC27A2,* all of which encode lipid metabolism-related proteins; the anti-apoptotic protein *BCL2-like1*; and *1-8D,* encoding a protein of unknown function.

Among the integrated genes, some (*AGT, FHS, 1-8D, FLC* and *GC*) were inserted into the host genome as a full-length coding sequence (CDS). As a result, these genes produced functional proteins that could be expressed in UT-7/EPO cells and lead to colony formation in the absence of EPO. Other genes (*BCL2-like1*, *APOA-1*, *PDPK1*, *FGL1*, *APOE*, *SLC27A2* and *COL18A1*) were inserted as a partial CDS that lacked the 5′ first start codons but contained 3′ stop codons, indicating that these genes were translated from a secondary start codon to the stop codon to yield partial proteins. As a result, functional proteins may be expressed in UT-7/EPO cells, leading to colony formation in the absence of EPO. The remaining inserted genes (*EBAG9*, *ABI-2*, *ASGR2* and *APOJ*) consisted of only a

Table 2 Gene specific primers for candidate genes in mice

Agt	5′	AGTGGGAGAGGTTCTCAATAGCA
	3′	GACGTGGTCGGCTGTTCCT
Ebag9	5′	GCAGCTACACAAGACATGCCTTT
	3′	TCCCACGCATTGCTATTTTCT
Bcl2-like1	5′	GGCTGGGACACTTTTGTGGAT
	3′	AAGCGCTCCTGGCCTTTC
Apoa-1	5′	GACAGCGGCAGAGACTATGTGT
	3′	AGGAGATTCAGGTTCAGCTGTTG
Fhs	5′	GCATGCCGAGAAACTGATGA
	3′	TCACGGTCTGGTTTCTTTATATCCT
Pdpk1	5′	TTCTTGGCGAGGGCTCTTT
	3′	CATATTCTCTGGAAGTGGCCAGTT
Abi-2	5′	GCGGGTGGCCGACTACT
	3′	TCTTCTAGGGCTCGCTGCTT
Apoe	5′	AGCTGCAGAGCTCCCAAGTC
	3′	TTACTTCCGTCATAGTGTCCTCCAT
1-8d	5′	CCTGGGCTTCGTTGCCTAT
	3′	CACATCGCCCACCATCTTC
Asgr2	5′	GGAGGAGAAGCAGCAACAGCTA
	3′	TGGGAAGTGCTTCAGGTGAAA
Flc	5′	CGGGCCTCCTACACCTACCT
	3′	GCCACGTCATCCCGATCA
Slc27a2	5′	CAACACACCGCAGAAACCAA
	3′	CCATTTCCCAGGGCTTTTTT
Rpl10	5′	TTCCATGTCATCCGTATCAACAA
	3′	CCCTGTCTGGAGCCTGTCA
Col18a1	5′	GCAGAGCCAGAGAATGTTGCT
	3′	CCCGACGTGAGGGTCATC
Apoj	5′	GGTCGGCCAGCAGCTAGAG
	3′	CGCCGTTCATCCAGAAGTAGA
Gc	5′	GGATCCTGCTGTACTTCTGCAA
	3′	TGCTTCATCTGGAGTCTCTCCTT

partial CDS without an open reading frame (ORF). These genes were translated from the shifted reading frame of the original mRNA and produced proteins of uncertain function. However, these genes resulted in UT-7/EPO colony formation in the absence of EPO. All of the 17 candidate cDNAs with full-length, partial or matched ORFs or partial but non-matched ORFs were examined in a secondary screen to identify specific genes that were involved in terminal erythroid maturation.

Expression of EPO-independent Growth-inducing Genes in Mouse FL Erythroid Populations

To determine which candidate genes obtained from first screen are critical for primary erythroid cell maturation, we performed a second screen to analyze gene expression during erythroid development. We used mouse fetuses for the second screen since mouse fetal samples are easier to obtain and use than human samples. The mouse homologues of these candidate genes were identified and the expression of the candidate genes was analyzed by RT-PCR using gene-specific primers (Table 2).

First, gene expression was assessed in samples from E10.5 whole embryos (WE) and E12.5 FL. All candidate genes were expressed in E12.5 FL with the exception of *Asgr-2,* which was eliminated as a gene of interest (Fig. 2). *Ebag9* and *Col18a1* expression was lower in the FL than in the whole E10.5 embryos, while *Fhs* and *Gc* had the opposite expression pattern with higher expression in the FL samples.

Next, we analyzed candidate gene expression in a series of FL-derived hematopoietic populations ranging from uncommitted hematopoietic stem cells (HSCs) to mature erythrocytes as determined by the expression of the surface markers CD45, Sca-1, c-Kit, CD71 and Ter119 (Fig. 3a). The following criteria were used to identify each hematopoietic population: (1) CD45+/Sca-1+/c-Kit+ cells represent HSCs; (2) c-Kit+ (Sca-1-/c-Kit+/CD71-/Ter119-) cells are BFU-E; (3) c-Kit+/CD71+ (Sca-1-/c-Kit+/CD71+/Ter119-) cells are committed erythroid progenitor cells or CFU-E; (4) CD71+/Ter119+ (Sca-1-/c-Kit-/CD71+/Ter119+) cells are proerythroblasts; and (5) Ter119+ (Sca-1-/c-Kit-/CD71-/Ter119+) cells represent mature erythroblasts and erythrocytes (Fig. 3a) [14, 15].

The mRNA expression of some candidate genes (*Abi-2*, *Slc27a2*) was higher in HSCs and gradually decreased throughout erythroid cell maturation (Fig. 3b). The expression of other candidate genes (*Pdpk1*, *Fhs*, *Flc*, *Rpl10*, *Ebag9* and *Apoe*) increased from HSCs to erythroblasts and then gradually decreased from erythroblasts to mature erythrocytes. *Bcl2l1* expression was low in HSCs and gradually increased. *Apoa-1* was highly expressed in

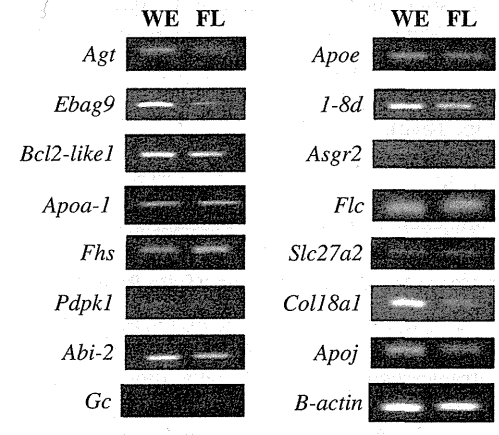

Fig. 2 Expression of candidate erythroid genes in developing mouse embryos. RT-PCR analyses of candidate genes in mouse embryos. We used RT-PCR to examine the expression patterns of the mouse homologues of each candidate gene in 10.5 dpc whole embryos (WE) and 12.5 dpc FL in ICR mouse embryos